The Journal of Experimental Biology 203,1459–1468 (2000)
Printed in Great Britain © The Company of Biologists Limited 2000
JEB2583

CENTRAL ROLE OF THE APICAL MEMBRANE H$^+$-ATPase IN ELECTROGENESIS AND EPITHELIAL TRANSPORT IN MALPIGHIAN TUBULES

KLAUS W. BEYENBACH[1,*], THOMAS L. PANNABECKER[2] AND WOLFRAM NAGEL[3]

[1]*Department of Biomedical Sciences, VRT 8014, Cornell University, Ithaca, NY 14853, USA,* [2]*Department of Physiology, University of Arizona College of Medicine, Tucson, AZ 85742, USA* and [3]*Department of Physiology, University of Munich, D-80336 Munich, Germany*

*e-mail: KWB1@Cornell.edu

Accepted 21 February; published on WWW 6 April 2000

Summary

The effects of bafilomycin A_1, a blocker of V-type H$^+$-ATPases, were investigated in Malpighian tubules of *Aedes aegypti*. Bafilomycin A_1 reduced rates of transepithelial fluid secretion and the virtual short-circuit current (vI_{sc}) with an IC_{50} of approximately 5 μmol l^{-1}. As vI_{sc} decreased, the electrical resistance increased across the whole epithelium and across the apical membrane, indicating effects on electroconductive pathways. Bafilomycin A_1 had no effect when applied from the tubule lumen, pointing to the relative impermeability of the apical membrane to bafilomycin A_1. Thus, bafilomycin A_1 must take a cytoplasmic route to its blocking site in the proton channel of the H$^+$-ATPase located in the apical membrane of principal cells. The inhibitory effects of bafilomycin A_1 were qualitatively similar to those of dinitrophenol in that voltages across the epithelium (V_t), the basolateral membrane (V_{bl}) and the apical membrane (V_a) depolarized towards zero in parallel. Moreover, V_{bl} always tracked V_a, indicating electrical coupling between the two membranes through the shunt. Electrical coupling allows the H$^+$-ATPase to energize not only the apical membrane, but also the basolateral membrane. Furthermore, electrical coupling offers a balance between electroconductive entry of cations across the basolateral membrane and extrusion across the apical membrane to support steady-state conditions during transepithelial transport.

Key words: vacuolar-type H$^+$-ATPase, bafilomycin, dinitrophenol, short-circuit current, apical membrane, insect, mosquito, *Aedes aegypti*, secretory epithelium.

Introduction

In the past, our laboratory has investigated the mechanisms of transepithelial electrolyte and fluid secretion in Malpighian tubules of the yellow fever mosquito *Aedes aegypti* by focusing on the mechanism and regulation of (i) Na^+ and K^+ entry across the basolateral membrane of principal cells, and (ii) Cl^- transport through the shunt pathway (Beyenbach, 1995). Greatly aided by the availability of bafilomycin, we have now begun to explore the role of the apical membrane of principal cells in transepithelial electrolyte secretion. This membrane is thought to be the site of a vacuolar H$^+$-ATPase, which in other insect epithelia is believed to energize secondary active electrolyte transport across membranes and whole epithelia (Harvey and Wieczorek, 1997; Wieczorek et al., 1999).

In the present study, we have found a bafilomycin-sensitive electrogenic pump, presumably a V-type H$^+$-ATPase, in the apical membrane of principal cells. The pump polarizes not only the apical membrane but also the basolateral membrane by virtue of electrical coupling through the shunt pathway. Electrical coupling allows the electrical driving forces at the basolateral and apical membranes to rise and fall in parallel so that cation entry across the basolateral membrane matches cation extrusion across the apical membrane.

Materials and methods

Mosquitoes and isolation of Malpighian tubules

Mosquitoes of the genus *Aedes aegypti* L. (NIH strain) were reared as described by Pannabecker et al. (1993). Adults were kept under a 12 h:12 h light:dark regimen and offered 3 % sucrose *ad libitum*. Only adult female mosquitoes between 3 and 6 days old were used for experiments. Malpighian tubules were dissected from cold-anaesthetized mosquitoes as described previously (Pannabecker et al., 1993).

Solutions

Mosquito Ringer's solution contained in (mmol l^{-1}): NaCl 150, KCl 3.4, $CaCl_2$ 1.7, $MgCl_2$ 0.6, $NaHCO_3$ 1.8, Hepes 25, and glucose 5. The pH was adjusted to 7.0 with NaOH. Bafilomycin A_1 was purchased from K. Altendorf (Osnabrück, Germany), dissolved in 100 % dimethyl sulfoxide (DMSO, Sigma) as 100 and 10 mmol l^{-1} stock solutions, and stored at

–20 °C until use. At the concentration of bafilomycin A_1 normally used (10^{-5} mol l^{-1}), the DMSO concentration was 0.01 % or 0.1 %, which had no effect on transepithelial fluid secretion in isolated Malpighian tubules.

Transepithelial fluid secretion

Rates of transepithelial fluid secretion were measured in isolated Malpighian tubules by the method of Ramsay adapted by our laboratory (Plawner et al., 1991). Six consecutive measurements of cumulative volume over time (30 min) yielded the fluid secretion rate, first in the absence (control) and then in the presence of bafilomycin A_1. Thus, each tubule served as its own control. The time course of the effect of bafilomycin A_1 on fluid secretion was evaluated by measuring secreted volume every 2 min after addition of the antibiotic to the peritubular bath.

Electrophysiological measurements

Isolated Malpighian tubules (0.3–0.6 mm long) were cannulated and perfused *in vitro* using methods described previously (Beyenbach and Frömter, 1985). The transepithelial voltage (V_t) was measured continuously *via* Ag/AgCl electrodes and 4 % Ringer/agar bridges positioned in the tubule lumen and the peritubular bath (ground). The basolateral membrane voltage of principal cells (V_{bl}) was measured using a conventional microelectrode filled with 850 mmol l^{-1} potassium acetate and 150 mmol l^{-1} potassium chloride. The apical membrane voltage of the principal cell (V_a) was calculated as the difference between V_t and V_{bl}. The transepithelial resistance, R_t, and the fractional resistance of the apical membrane, fR_a, were measured by cable analysis (Helman, 1972), except that we used a double-barrelled perfusion pipette to separate current injection into the tubule lumen through one barrel (100–500 nA, 300 ms) from the measurement of transepithelial voltage through the other (Beyenbach and Frömter, 1985).

Each perfused tubule served as its own control. The flow rate of Ringer's solution through the peritubular bath was 0.5 ml min^{-1} at steady state and increased briefly to 4 ml min^{-1} when the peritubular Ringer's solution was changed to include bafilomycin A_1. The tubule lumen was perfused with Ringer's solution through the voltage barrel of a double-barrelled perfusion pipette at rates between 1 and 5 nl min^{-1}. An exchange pipette lodged in the voltage barrel served to change the luminal perfusion fluid rapidly.

Electrophysiological data are interpreted on the basis of the Ussing–Windhager model (1964) of epithelial ion transport (Fig. 1). The circuit model uses a minimum number of components to account for the transepithelial voltage V_t and resistance R_t: the transcellular resistance R_c, the shunt resistance R_{sh} and the electromotive force of the transcellular active transport pathway E_c. The requirement for energy input (ATP) confines the active transport pathway (consisting of E_c and R_c) to epithelial cells which, in the case of *Aedes aegypti* Malpighian tubules, are the principal cells. The shunt pathway is located outside principal cells (Fig. 1). It may be the paracellular pathway through septate junctions (Pannabecker et al., 1993) or a pathway through stellate cells (O'Donnell et al., 1998). The cations Na^+ and K^+ are secreted from the haemolymph to the tubule lumen *via* the active transport pathway, and Cl^- is secreted *via* the shunt pathway (Beyenbach, 1995).

During *in vitro* microperfusion of the tubule lumen with the same Ringer's solution as is present in the peritubular bath (symmetrical condition), current I passing through transcellular (R_c) and shunt (R_{sh}) resistances is:

$$I = \frac{E_c}{R_c + R_{sh}} \quad . \tag{1}$$

The transepithelial voltage is:

$$V_t = IR_{sh} = \frac{E_c R_{sh}}{R_c + R_{sh}} \quad . \tag{2}$$

The transepithelial resistance is:

$$R_t = \frac{R_c R_{sh}}{R_c + R_{sh}} \quad . \tag{3}$$

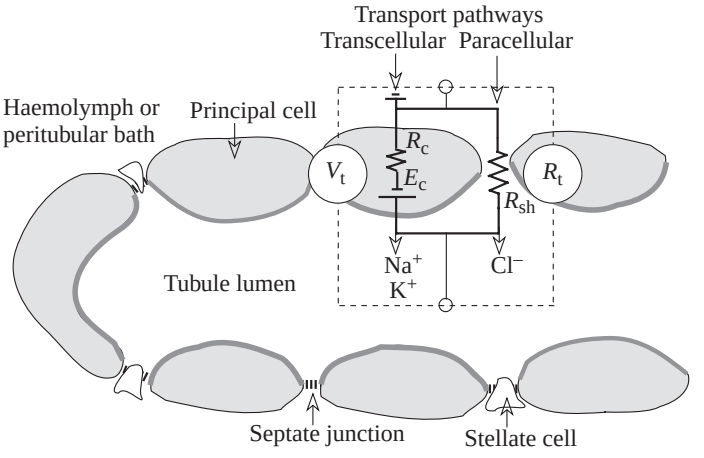

Fig. 1. The Ussing–Windhager model of transepithelial ion transport across electrogenic epithelia as applied to ion secretion in Malpighian tubules of *Aedes aegypti*. There are two types of epithelial cell: principal and stellate. Principal cells are the sites of the active transport pathway modelled as the electromotive force (E_c) for transcellular cation transport in series with the transcellular resistance R_c. Stellate cells and/or the paracellular pathway may be the site of the shunt pathway, R_{sh}. Cationic current (Na^+, K^+) flowing through the active transport pathway is equivalent to anionic current (Cl^-) flowing through the shunt pathway, bringing about transepithelial secretion of NaCl and KCl. V_t, transepithelial voltage; R_t, transepithelial resistance.

It follows that the ratio V_t/R_t is the virtual short-circuit current vI_{sc}.

$$vI_{sc} = \frac{V_t}{R_t} = \frac{E_c}{R_c} . \quad (4)$$

Since, in the present study, the short-circuit current is calculated as the ratio of the transepithelial voltage to the resistance, it is called the 'virtual short-circuit current', vI_{sc}, to indicate that it is not measured directly by transepithelial voltage-clamping to 0 mV (which is not easily done in tubular epithelia). Nevertheless, vI_{sc} is an estimate of the maximum rate of active transport through the cell if the shunt resistance were replaced with zero resistance and thereby 'short-circuited'.

In addition to the transepithelial resistance, which is the radial resistance of the tubule, cable analysis yields the core resistance, R_{core}, which is the axial resistance of the tubule:

$$R_{core} = \frac{4\sigma}{\pi(D_e)^2} , \quad (5)$$

where σ is the resistivity of the Ringer's solution in the tubule lumen (74 Ωcm) and D_e is the electrical diameter of the core. Thus, D_e can be calculated from R_{core} and compared with the optical diameters (inner and outer) of the tubule. Principal cells obstruct the view of the tubule lumen, but thin, transparent stellate cells do not.

Electrical circuit analysis (Yonath–Civan plots)

Since conductance is the inverse of resistance, transepithelial conductance, g_t, is:

$$g_t = g_c + g_{sh} , \quad (6)$$

where g_c is the transcellular conductance and g_{sh} is the shunt conductance. Moreover,

$$g_c = \frac{I_{sc}}{E_c} . \quad (7)$$

Substitution yields the equation of a line with slope of $1/E_c$ and with g_{sh} as intercept (see Fig. 6).

$$g_t = \frac{1}{E_c} I_{sc} + g_{sh} . \quad (8)$$

Yonath and Civan (1971) first used this approach in toad bladder to estimate the electromotive force of the active transport pathway and the shunt resistance. Although the estimate of E_c gives no information about the mechanism of its generation, it is useful in providing some idea of the driving forces (Helman and Thompson, 1982).

Statistical treatment of the data

The statistical significance of the data was evaluated with Student's *t*-test for paired data (each tubule serving as its own control) and for unpaired data (comparisons of sample means with unequal variances). Values are presented as means ± S.E.M.

Results

Effects of peritubular bafilomycin A_1 on transepithelial fluid secretion and short-circuit current

The inhibitory effects of bafilomycin A_1 (10^{-5} mol l^{-1}) on rates of transepithelial fluid secretion and on virtual short-circuit current (vI_{sc}) developed gradually (Fig. 2). The mean rate of transepithelial fluid secretion was 0.62±0.05 nl min^{-1} in 13 Malpighian tubules, each serving as its own control. After adding bafilomycin A_1 to the peritubular Ringer, rates of fluid secretion began to decline and reached 60 % inhibition 40 min later. Complete (100 %) inhibition of transepithelial fluid secretion was not observed in the presence of 10^{-5} mol l^{-1} bafilomycin A_1, but it was observed in some tubules at a concentration of 5×10^{-5} mol l^{-1}.

Inhibition of vI_{sc} roughly paralleled the inhibition of fluid secretion (Fig. 2). The virtual short-circuit current, a measure of active transport, was 6.44 μA cm^{-1} under control conditions in nine Malpighian tubules (Table 1). Upon addition of bafilomycin A_1 (10^{-5} mol l^{-1}) to the peritubular Ringer, vI_{sc} started a progressive decline that reached 70 % inhibition 30 min later (Fig. 2). Short exposures to peritubular bafilomycin A_1 (5–10 min) were reversible; longer exposures (15 min and longer) were not (data not shown). 'Complete inhibition' of vI_{sc} was observed only after the sudden collapse of the transepithelial voltage and resistance that presumably reflects the toxic effects of bafilomycin A_1 (see Fig. 5).

Dose–response curves for peritubular bafilomycin A_1

Dose–response curves for bafilomycin A_1 were assessed between 10 and 40 min of exposure to the antibiotic, or shortly before voltages and resistances collapsed to values close to

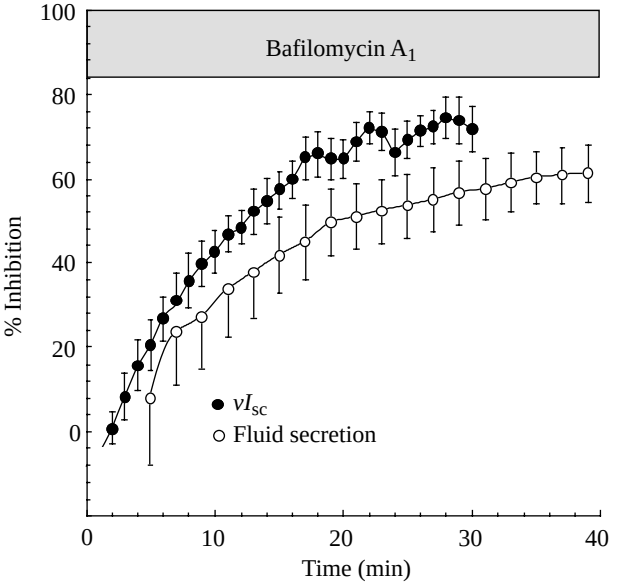

Fig. 2. Time course of the inhibitory effects of bafilomycin A_1 (10^{-5} mol l^{-1}) on the virtual short-circuit current, vI_{sc}, in nine isolated perfused Malpighian tubules and on rates of transepithelial fluid secretion in 13 Malpighian tubules. Values are means ± S.E.M.

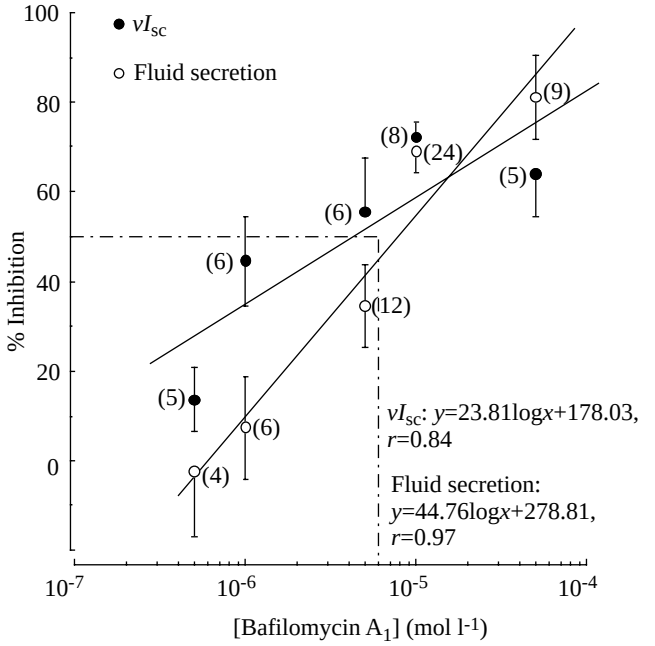

Fig. 3. Dose-dependence of the bafilomycin A_1 inhibition of the virtual short-circuit current (vI_{sc}; filled circles) and transepithelial fluid secretion (open circles) in Malpighian tubules of *Aedes aegypti*. Values are given as the mean ± S.E.M., with the number of Malpighian tubules in parentheses.

zero (see Fig. 5). Fig. 3 shows that peritubular bafilomycin A_1 had little or no effect on transepithelial fluid secretion and vI_{sc} at concentrations below 4×10^{-7} mol l^{-1}. Inhibitory effects became significant ($P<0.05$) at a concentration of 10^{-6} mol l^{-1} and reached 50 % inhibition at a concentration of approximately 5×10^{-6} mol l^{-1} (Fig. 3). The correlation coefficient for the effects on fluid secretion (r=0.97) was higher than that for the effects on virtual short-circuit current (r=0.84).

Polar effects of bafilomycin A_1 and dinitrophenol

In vitro microperfusion of Malpighian tubules allows solution changes in the tubule lumen. The act of perfusing the lumen can be confirmed by visual inspection of fluid rising in the pipette holding the distal end of the tubule. Application of bafilomycin A_1 to the tubule lumen had no effect on transepithelial voltage and resistance (Fig. 4A). In contrast, application of bafilomycin A_1 from the peritubular side depolarized the transepithelial voltage while increasing transepithelial resistance (Fig. 4B). Similar results were obtained with three additional Malpighian tubules (not shown).

The effect of another inhibitor, dinitrophenol (DNP), on transport across Malpighian tubules showed similar polarity. Dinitrophenol added to peritubular Ringer is known to depolarize transepithelial voltage and to increase

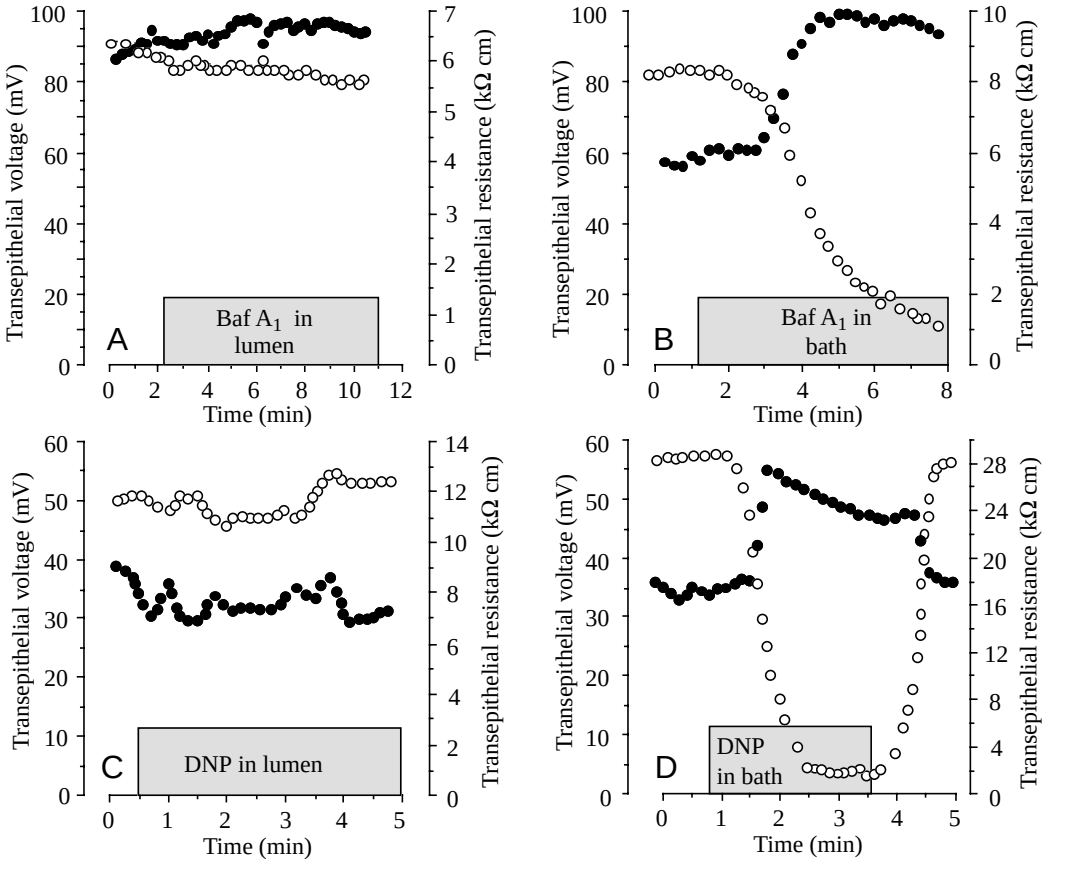

Fig. 4. Effects of bafilomycin A_1 (10^{-5} mol l^{-1}) (A,B) and dinitrophenol (DNP; 10^{-4} mol l^{-1}) (C,D) in isolated perfused Malpighian tubules of *Aedes aegypti*. Bafilomycin A_1 and dinitrophenol had effects on transepithelial voltage (open circles) and resistance (filled circles) when presented from the peritubular bath (B,D) but not from the tubule lumen (A,C).

Table 1. *Effects of bafilomycin A_1 on electrophysiological variables in isolated perfused Malpighian tubules of* Aedes aegypti

	Transepithelial voltage, V_t (mV)	Transepithelial resistance, R_t (kΩ cm)	Vitual short-circuit current, vI_{sc} (μA cm^{-1})	Basolateral membrane voltage, V_{bl} (mV)	Apical membrane voltage, V_a (mV)	Core resistance, R_{core} (MΩ cm)	Fractional resistance, apical membrane, fR_a	Electrical diameter of tubule, D_e (μm)
Control	46.4±4.6	7.77±1.32	6.44±0.50	−79.6±3.8	126.0±5.5	16.39±4.81	0.27±0.03	29.8±4.0
Bafilomycin	18.2±3.5	11.61±2.21	1.67±0.25	−17.7±6.4	35.9±8.7	24.38±7.39	0.57±0.03	24.7±3.3
P	<0.00006	<0.004	<0.000007	<0.00001	<0.00000008	<0.026	<0.000005	<0.0014

The effects of bafilomycin A_1 (10^{-5} mol l^{-1}) were assessed between 10 and 40 min after the addition of bafilomycin to the peritubular Ringer bath and always shortly before voltages and resistances collapsed to zero (see Fig. 5).

Values are means ± S.E.M. (N=9).

Table 2. *Yonath–Civan (Y-C) estimates of the shunt and transcellular resistance and of the electromotive force of the active transport pathway in 14 Malpighian tubules of* Aedes aegypti

	Transepithelial voltage (mV)	Transepithelial resistance (kΩ cm)	Y-C estimate of shunt conductance (μS cm^{-1})	Y-C estimate of shunt resistance (kΩ cm)	Y-C estimate of the EMF of the active transport pathway (mV)	Y-C estimate of transcellular resistance (kΩ cm)	Correlation coefficient of Y-C plots, r
	61.2	14.8	20.2	49.6	87.8	21.0	0.993
	61.2	12.8	39.1	25.6	126.0	25.6	0.961
	64.5	18.3	24.7	40.5	92.2	33.4	0.986
	89.3	7.6	75.3	13.3	201.7	17.8	0.983
	22.6	4.9	113.1	8.8	50.0	11.0	0.993
	62.7	9.6	30.0	33.4	78.7	13.5	0.979
	52.5	5.8	110.7	9.0	180.5	16.2	0.813
	32.4	6.5	91.7	10.9	88.0	16.1	0.964
	41.8	5.1	104.4	9.6	88.0	10.9	0.964
	64.4	12.2	42.5	23.5	149.9	25.4	0.927
	88.7	6.1	77.2	13.0	166.9	11.5	0.985
	38.7	4.7	72.2	13.9	61.1	7.1	0.993
	52.4	8.6	32.6	30.7	73.8	11.9	0.991
	41.9	5.8	131.5	7.6	197.9	24.5	0.762
Mean ± S.E.M.	55.3±5.3	8.77±1.17	68.9±10.4	20.67±3.73	117.3±14.5	17.6±2.1	0.949±0.020

EMF, electromotive force.

transepithelial resistance (Pannabecker et al., 1992). In the present study, we extended these findings to show that DNP, like bafilomycin A_1, had no effect when presented from the tubule lumen (Fig. 4C), but was effective when added to the peritubular bath (Fig. 4D).

Effects of bafilomycin A_1 on principal cells of Malpighian tubules

Details of the inhibitory effects of bafilomycin A_1 on the electrophysiological correlates of transepithelial transport were studied in nine perfused Malpighian tubules (Table 1). Fig. 5 illustrates a representative experiment in which, under control conditions, the transepithelial voltage was 61.2 mV (lumen-positive), the apical membrane voltage was 142.8 mV (lumen-positive) and the basolateral membrane voltage was 81.6 mV (cell-negative). After the addition of bafilomycin A_1 to the peritubular bath, all voltages began to decline towards zero as the transepithelial resistance increased (Fig. 5). The virtual short-circuit current decreased in parallel, indicating the progressive inhibition of transcellular active transport. After exposure to bafilomycin A_1 for approximately 35 min, all voltages suddenly collapsed to zero in parallel with a drop in the transepithelial resistance. Accordingly, the effects of bafilomycin A_1 can be divided into two phases: (i) inhibitory effects that increase gradually over the course of 30 min or less, followed by (ii) an irreversible loss of all voltages and the transepithelial resistance.

The initial inhibitory effects of bafilomycin A_1 on transcellular transport (fall of vI_{sc}) are paralleled by an increase in the fractional resistance of the apical membrane and a decrease in the electrical diameter of the tubule (Fig. 5). These effects signal a shift of the transepithelial resistance towards the apical membrane, the site of the H^+-ATPase. The irreversible collapse of voltage and resistance after 35 min of bafilomycin A_1 treatment probably reflects toxic effects. Bafilomycin A_1 inhibits not only the H^+-ATPase in the apical membrane, but also in endosomes, vacuoles and other cell organelles. Inhibition of these H^+-ATPases could contribute to the sudden collapse of voltages and resistances.

Observations made in all nine Malpighian tubules are summarized in Table 1, which shows data collected in the absence (control) and in the presence of bafilomycin A_1 shortly before voltages and resistance collapsed. Bafilomycin A_1 had significant effects on every electrophysiological indicator of transepithelial transport (Table 1). Virtual short-circuit current and all voltages (membrane and transepithelial) dropped to values less than 40 % of control values, while transepithelial resistance increased by 34 %. Measurements of fractional resistance indicated that, under control conditions, the apical membrane is the site of 27 % of the transcellular resistance, leaving 73 % to the basolateral membrane of principal cells (Table 1). In the presence of bafilomycin A_1, this distribution shifts, with 57 % of the transecellular resistance relocating at the apical membrane, leaving 43 % to the basolateral membrane. The shift of resistance to the apical membrane is confirmed in measurement of the core resistance, which

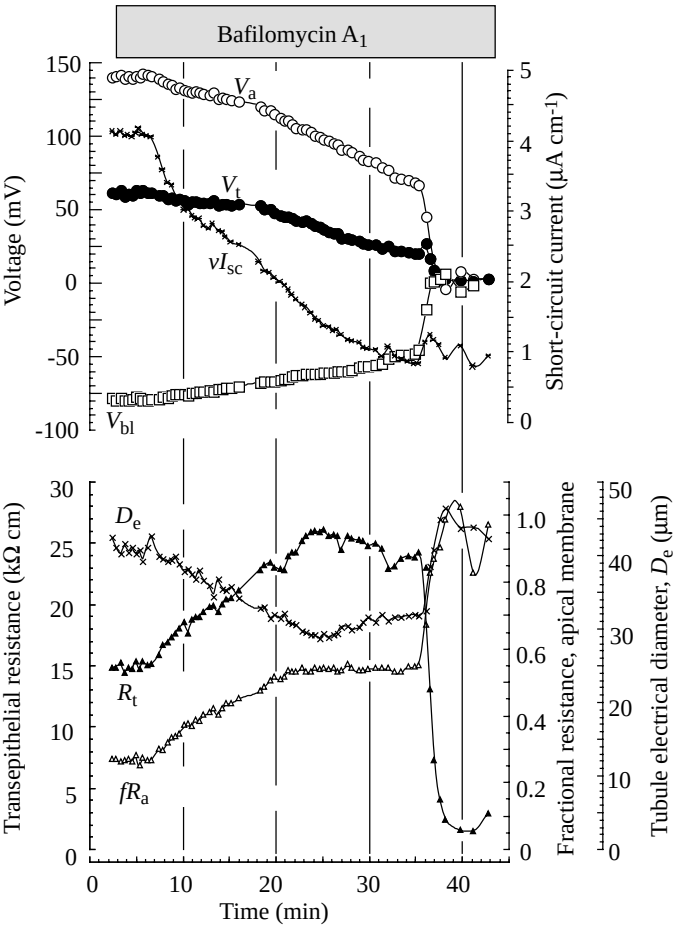

Fig. 5. The effects of bafilomycin A_1 (10^{-5} mol l^{-1}) on electrophysiological variables in a representative Malpighian tubule perfused with the same Ringer's solution present in the peritubular bath. After the addition of bafilomycin A_1 to the peritubular bath, transepithelial voltage V_t (filled circles), apical membrane voltage V_a (open circles) and basolateral membrane voltage V_{bl} (open squares) began to decline towards zero accompanied by a decrease in the virtual short-circuit current vI_{sc} (crosses, upper panel). In parallel, transepithelial resistance R_t (filled triangles) and the fractional resistance of the apical membrane fR_a (open triangles) increased, while tubule electrical diameter D_e (crosses) decreased (lower panel). After 35 min, all voltages and the transepithelial resistance collapsed to values close to zero.

increases by 48 % in the presence of bafilomycin A_1, indicating a decrease in the electrical diameter of the tubule (Table 1).

Equivalent circuit analysis (Yonath–Civan estimates) of electromotive force and shunt conductance

Dose-dependent or time-dependent effects of stimulators or inhibitors of transport can be used according to the protocol suggested by Yonath and Civan (1971) to estimate epithelial shunt conductance and the electromotive force of the active transport pathway. Such a plot of vI_{sc} *versus* transepithelial conductance (as a function of time in bafilomycin A_1) is shown in Fig. 6, yielding a shunt conductance of 20.2 μS cm^{-1} (shunt

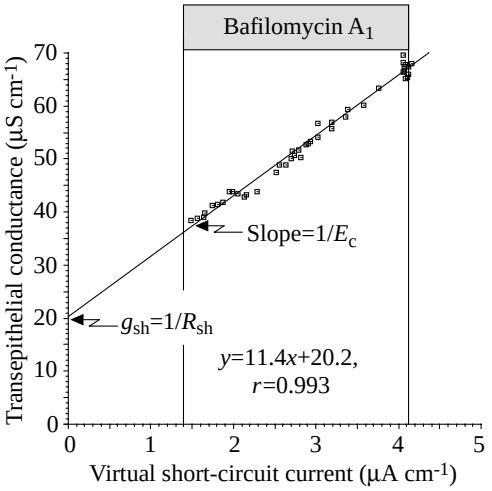

Fig. 6. Yonath–Civan plot of virtual short-circuit current (vI_{sc}) *versus* transepithelial conductance in a representative Malpighian tubule perfused with the same Ringer's solution present in the peritubular bath. The *y*-intercept is the shunt conductance (g_{sh}), and the slope is the inverse of the electromotive force of the transcellular active transport pathway (E_c). R_{sh}, shunt resistance.

resistance 49.6 kΩ cm) and 87.8 mV as the electromotive force (E_c) of the active transport pathway. Table 2 summarizes similar Yonath–Civan estimates taken in all 14 tubule experiments. This summary yields a mean shunt resistance of 20.7 kΩ cm, a mean transcellular resistance of 17.6 kΩ cm and a mean electromotive force of the active transport pathway of 117.3 mV (Table 2; Fig. 7).

Discussion

The virtual short-circuit current

In vitro microperfusion is the method of choice for measuring electrophysiological correlates of ion transport across Malpighian tubules. The ratio of the transepithelial voltage to the transepithelial resistance yields the virtual short-circuit current, which is a measure of the rate of active transport of Na^+ and K^+ into the tubule lumen (equation 4). It is a virtual current because it is calculated from open-circuit measurements of transepithelial voltage and resistance rather than from real measurements of current at the transepithelial voltage-clamp of 0 mV. The virtual short-circuit current is an estimate of the maximum rate of active transport that would be possible if transepithelial electrolyte movement were not hindered by the resistance Cl^- encounters during transport through the shunt (Fig. 1; equation 4). The great advantage of measuring virtual short-circuit current is that effects on the active transport pathway can be observed while the experiment is in progress with greater resolution than that afforded by measurements of ion flux.

Role of apical membrane vacuolar H⁺-ATPase in transepithelial transport

Vacuolar-type H^+-ATPases are proton pumps that generate

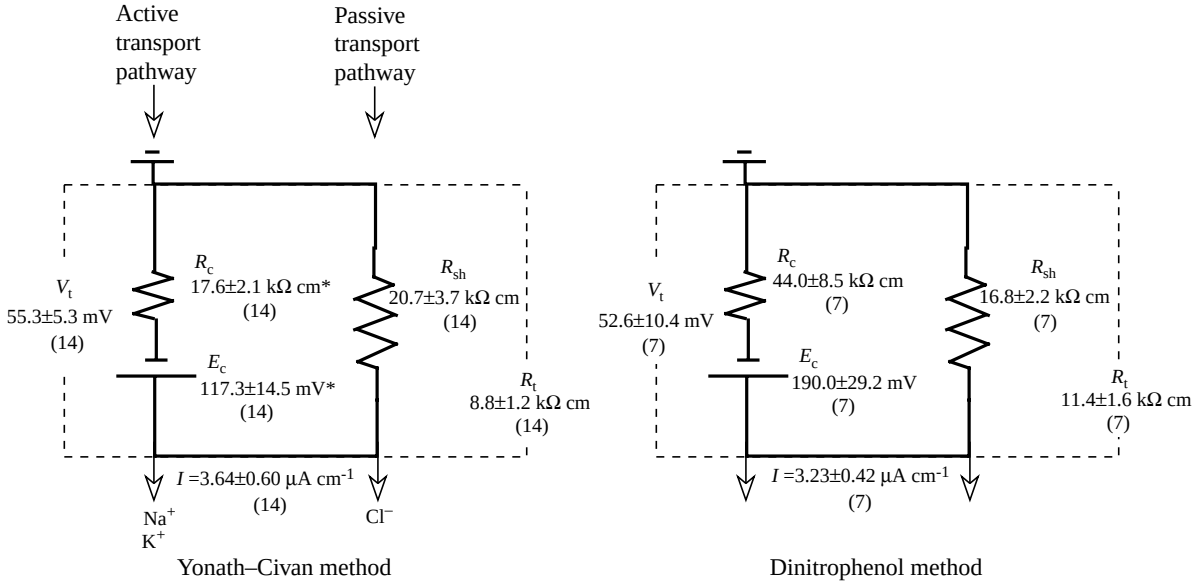

Fig. 7. Estimates of the circuit components of active and passive transport pathways that model transepithelial secretion of NaCl and KCl across Malpighian tubules of *Aedes aegypti*. The shunt resistance R_{sh} and the electromotive force of the active transport pathway (E_c) can be estimated from so-called Yonath–Civan plots (see Fig. 6). The shunt resistance can also be estimated by increasing transcellular resistance (R_c) to such a degree that transepithelial resistance approaches R_{sh}, as in a previous study using dinitrophenol (Pannabecker et al., 1992). Control values of E_c and R_c are then determined *via* circuit analysis. Comparing the results of the two methods: estimates of R_{sh} are similar, but Yonath–Civan estimates of E_c and R_c are significantly lower ($P<0.05$) than those made using dinitrophenol. The results of the dinitrophenol method are taken from Pannabecker et al. (1992). V_t, transepithelial voltage; R_t, transepithelial resistance; *I*, intraepithelial current, $E_c/(R_c+R_{sh})$. *Significantly ($P<0.05$) different from the value using the dinitrophenol method.

large voltages across the membranes in which they are found. The molecular constituents of the pump are a cytoplasmic catalytic V_1 complex that utilizes ATP and a transmembranous V_o complex that functions as a proton channel (Merzendorfer et al., 1997). The V_1 and V_o complexes may associate and dissociate, which is thought to be under genetic regulation at the transcriptional and post-transcriptional levels (Wieczorek et al., 1999).

Bafilomycin A_1 inhibits H^+-ATPases by blocking the proton channel of the pump (Crider et al., 1994; Gill et al., 1998; Peng et al., 1999). In the present study, inhibition of the virtual short-circuit current was observed when bafilomycin A_1 was presented from the peritubular side but not when it was present on the luminal side (Fig. 4). Hence, bafilomycin A_1 does not block the proton channel from its opening into the tubule lumen, but gains access to its blocking site from the cytoplasm, after permeation of the basolateral membrane (Fig. 4).

The bafilomycin A_1 inhibition of both short circuit-current and transepithelial fluid secretion illustrates the central role of proton conduction through the H^+-ATPase in powering salt and water transport across Malpighian tubules (Fig. 2). The short-circuit current reflects energy-dependent transport of Na^+ and K^+ through principal cells (Fig. 1). Na^+ and K^+ enter principal cells *via* channel- and carrier-mediated pathways (Sawyer and Beyenbach, 1985; Hegarty et al., 1991, 1992). Extrusion of Na^+ and K^+ from the cell is thought to be energized by the H^+-ATPase located in the apical membrane, i.e. the luminal brush border (Fig. 7). According to the model advanced by Harvey, Wieczorek and coworkers, the H^+-ATPase mediates the primary active transport step of translocating protons into the extracellular space, the tubule lumen in the case of *Aedes aegypti* Malpighian tubules (Harvey and Wieczorek, 1997; Wieczorek et al., 1991; Wieczorek, 1992; Lepier et al., 1994). The H^+ electrochemical potential thus generated across the apical membrane powers secondary active transport of Na^+ and K^+ into the lumen *via* H^+/Na^+ and H^+/K^+ antiport with stoichiometries that have yet to be determined for *Aedes aegypti* Malpighian tubules. Interference in the active transport of protons, by depriving the H^+-ATPase of ATP (treatment with dinitrophenol) or by blocking the proton channel of the H^+-ATPase with bafilomycin A_1, inhibits (i) current generation at the apical membrane, (ii) secondary active transport of Na^+ and K^+ across the apical membrane, and (iii) intraepithelial current and, hence Cl^- transport, through the shunt (Fig. 1). The result is inhibition of transepithelial electrolyte and water transport.

The bafilomycin A_1 concentration that inhibits 50 % of the short-circuit current and transepithelial fluid secretion (IC_{50}), is 5 μmol l^{-1}, which is high in comparison with the nanomolar IC_{50} concentrations measured in other cells (Kohn et al., 1993; Ohta et al., 1998). However, the IC_{50} measured in the present study is based on bafilomycin A_1 concentrations in the extracellular medium and not on intracellular concentrations, where the antibiotic is active. Measuring a similar high IC_{50} in Malpighian tubules of ants, Dijkstra et al. (1994) concluded that the H^+-ATPase is only weakly bafilomycin-sensitive, which may also be true for *Aedes aegypti* Malpighian tubules. The need for high extracellular concentrations of bafilomycin A_1 in Malpighian tubules may also reflect poor permeation through plasma membranes, as suggested by the inability of bafilomycin A_1 to affect the virtual short-circuit current when the antibiotic is presented from the tubule lumen (Fig. 4). The unusual permeability properties of the brush-border apical membrane of *Aedes aegypti* Malpighian tubules are further documented by the failure of DNP to exert effects from the extracellular environment of the tubule lumen (Fig. 4). A low permeability of the apical membrane to bafilomycin was also noted in Malpighian tubules of the ant *Formica polyctena* (Weltens et al., 1992).

The inhibition of electrolyte and water transport is immediate and reversible when DNP is used to block ATP synthesis (Pannabecker et al., 1992). The inhibition by bafilomycin A_1 is slow, gradual and later irreversible (Figs 2, 5). The difference in time course could be related to differences in membrane permeability for bafilomycin A_1 and DNP, the latter being notably more permeable across the basolateral membrane. Significantly, the inhibition of the virtual short-circuit current by both DNP and bafilomycin A_1 is accompanied by a significant increase in transepithelial resistance that includes the increase in resistance of the apical membrane where the H^+-ATPase is located (Fig. 5; Table 1). Blocking the proton channel of the H^+-ATPase is expected to increase apical membrane resistance, which is reflected in an increase of apical membrane fractional resistance, fR_a (Table 1). Depriving the H^+-ATPase of ATP should not, in itself, alter the conductance of the associated pathway. Nevertheless, the fact that similar inhibition is caused by agents differing widely in their mechanisms of action, channel block by bafilomycin A_1 and inhibition of ATP synthesis by DNP, documents the central role of the apical membrane V-ATPase in transepithelial electrolyte and fluid secretion in Malpighian tubules.

Estimates of model circuit parameters

In a previous study, we used dinitrophenol (DNP) to inhibit transcellular transport and to increase transcellular resistance to such a degree that measurements of the transepithelial resistance approach the resistance of the shunt (Pannabecker et al., 1992). This strategy yielded a shunt resistance of 16.8 kΩ cm (Fig. 7). In the present study, we used bafilomycin A_1 and applied the method of Yonath and Civan (1971) to estimate a shunt resistance of 20.7 kΩ cm, which is not significantly different (P=0.41) from that measured with DNP (Pannabecker et al., 1992). In contrast, the estimate of the transcellular resistance by the method of Yonath and Civan was significantly (P=0.05) lower (17.6 kΩ cm) than R_c estimated using DNP (44.0 kΩ cm), suggesting that DNP blocks electroconductive pathways in addition to those blocked by bafilomycin (Fig. 7). The Yonath–Civan estimate of the electromotive force (117.3 mV) of the active transport pathway (E_c) was also significantly lower (P=0.04) than E_c estimated using the DNP method (190.0 mV) (Fig. 7). Again, DNP and

bafilomycin may affect targets they do not share, hence the different estimates of R_c and E_c. However, in spite of these differences, the effects of DNP and bafilomycin on the active transport pathway are large enough to yield similar estimates of the shunt resistance (Fig. 7).

Role of apical membrane vacuolar ATPase in voltage generation

Dinitrophenol reduces transepithelial voltage and voltages across basolateral and apical membranes of principal cells to values close to or indistinguishable from zero (Pannabecker et al., 1992). The tubule does not appear to suffer adverse effects in spite of the abolition of active transport and all voltages. For one reason, the effects of DNP on voltage and resistance are fully reversible upon washout (Pannabecker et al., 1992, 1993). For another reason, receptor-mediated mechanisms, such as that of leucokinin-VIII, remain intact in the presence of DNP (Pannabecker et al., 1993).

The nullification of apical and basolateral membrane voltages in the presence of DNP without a trace of ionic diffusion potentials has been an enigma to us since we first made this observation (Pannabecker et al., 1992) because it implies the absence of Na^+ and K^+ diffusion potentials across the basolateral membrane of principal cells after DNP treatment, despite their unquestionable presence under control conditions (Sawyer and Beyenbach, 1985). Although the effects of bafilomycin A_1 are not as quick, they are qualitatively similar to those of DNP (Fig. 4). The similarities allude to mechanisms of electrogenesis that in H^+-ATPase-supported systems are markedly different from those in Na^+/K^+-ATPase-supported systems. In cells supported largely by the Na^+/K^+-ATPase, the pump generates electrochemical potential differences for Na^+ and K^+ across plasma membranes that are subsequently used to produce membrane voltages (*via* K^+ channels) and to power carriers (electrogenic or neutral) such as Na^+/H^+ exchange, Na^+/glucose cotransport, Na^+/Ca^{2+} exchange, etc. In cells supported largely by H^+-ATPases, the pump generates electrochemical potential differences for H^+ that can subsequently be used to power H^+/Na^+ exchange and other H^+-based carriers (Wieczorek, 1992; Bertram and Wessing, 1994). More importantly, voltage is generated by the H^+-ATPase itself in the process of transporting H^+ alone. The H^+-ATPase is therefore electrogenic, generating large voltages in those membranes where they are located.

Wieczorek et al. (1991) have long proposed that V-ATPases energize the membranes in which they are located. The present study extends this proposition, by way of electrical coupling, to membranes not containing V-ATPases. In the case of the Malpighian tubules of *Aedes aegypti*, the apical membrane is electrically coupled to the basolateral membrane *via* a shunt pathway that has a resistance similar to that of the transcellular pathway (Fig. 7). The situation is similar in the Malpighian tubules of ants, in which current generated by the pump in the apical membrane flows through the shunt pathway and returns to the apical membrane *via* the basolateral membrane to complete the intraepithelial current loop (Weltens et al., 1992). The transepithelial voltage is therefore the product of current times shunt resistance and, hence, is lumen-positive. The basolateral membrane voltage is the product of the current and the basolateral membrane resistance plus or minus any electromotive force associated with that membrane. In *Aedes aegypti* Malpighian tubules, the principal determinant of cell-negative voltages across the basolateral membrane is the product of current and basolateral membrane resistance, with the current coming from the apical membrane through the shunt (Pannabecker et al., 1992; Beyenbach, 1995). Electrical coupling of apical and basolateral membranes explains the parallel changes in V_a, V_{bl} and V_t as they approach or reach zero in the presence of bafilomycin A_1 or DNP (Fig. 5). Moreover, V_t and V_{bl} are always less than V_a, which they track (Fig. 5), revealing the apical membrane H^+-ATPase as the source of intraepithelial current that is central to transepithelial transport and to electrogenesis at both membranes of principal cells.

The authors thank the National Science Foundation for enabling this study (IBN 9604394).

References

Bertram, G. and Wessing, A. (1994). Intracellular pH regulation by the plasma membrane V-ATPase in Malpighian tubules of *Drosophila* larvae. *J. Comp. Physiol.* B **164**, 238–246.

Beyenbach, K. W. (1995). Mechanisms and regulation of epithelial transport across Malpighian tubules. *J. Insect Physiol.* **41**, 197–207.

Beyenbach, K. W. and Frömter, E. (1985). Electrophysiological evidence for Cl^- secretion in shark proximal tubules. *Am. J. Physiol.* **248**, F282–F295.

Crider, B. P., Xie, X. S. and Stone, D. K. (1994). Bafilomycin inhibits proton flow through the H^+ channel of vacuolar proton pumps. *J. Biol. Chem.* **269**, 17379–17381.

Dijkstra, S., Lohrmann, E., Van Kerkhove, E. and Greger, R. (1994). Characteristics of the luminal proton pump in Malpighian tubules of the ant. *Renal Physiol. Biochem.* **17**, 27–39.

Gill, S. S., Chu, P. B., Smethurst, P., Pietrantonio, P. V. and Ross, L. S. (1998). Isolation of the V-ATPase A and c subunit cDNAs from mosquito midgut and Malpighian tubules. *Arch. Insect Biochem. Physiol.* **37**, 80–90.

Harvey, W. R. and Wieczorek, H. (1997). Animal plasma membrane energization by chemiosmotic H^+ V-ATPases. *J. Exp. Biol.* **200**, 203–216.

Hegarty, J. L., Zhang, B., Carroll, M. C., Cragoe, E. J. and Beyenbach, K. W. (1992). Effects of amiloride on isolated Malpighian tubules of the yellow fever mosquito. *J. Insect Physiol.* **38**, 329–337.

Hegarty, J. L., Zhang, B., Pannabecker, T., Petzel, D. H., Baustian, M. D. and Beyenbach, K. W. (1991). Dibutyryl cAMP activates bumetanide-sensitive electrolyte transport in Malpighian tubules. *Am. J. Physiol.* **261**, C521–C529.

Helman, S. I. (1972). Determination of electrical resistance of the isolated cortical collecting tubule and its possible anatomical location. *Yale J. Biol. Med.* **45**, 339–345.

Helman, S. I. and Thompson, S. M. (1982). Interpretation and use of electrical equivalent circuits in studies of epithelial tissues. *Am. J. Physiol.* **243**, F519–F531.

Kohn, O. F., Mitchell, P. P. and Steinmetz, P. R. (1993). Sch-28080 inhibits bafilomycin-sensitive proton secretion in turtle bladder independently of luminal potassium. *Am. J. Physiol.* **265**, F174–F179.

Lepier, A., Azuma, M., Harvey, W. R. and Wieczorek, H. (1994). K^+/H^+ antiport in the tobacco hornworm midgut: the K^+-transporting component of the K^+ pump. *J. Exp. Biol.* **196**, 361–373.

Merzendorfer, H., Graf, R., Huss, M., Harvey, W. R. and Wieczorek, H. (1997). Regulation of proton-translocating V-ATPases. *J. Exp Biol.* **200**, 225–235.

O'Donnell, M. J., Rheault, M. R., Davies, S. A., Rosay, P., Harvey, B. J., Maddrell, S. H. P., Kaiser, K. and Dow, J. A. T. (1998). Hormonally controlled chloride movement across *Drosophila* tubules is *via* ion channels in stellate cells. *Am. J. Physiol.* **274**, R1093–R1049.

Ohta, T., Arakawa, H., Futagami, F., Fushida, S., Kitagawa, H., Kayahara, M., Nagakawa, T., Miwa, K., Kurashima, K., Numata, M., Kitamura, Y., Terada, T. and Ohkuma, S. (1998). Bafilomycin A1 induces apoptosis in the human pancreatic cancer cell line Capan-1. *J. Path.* **185**, 324–330.

Pannabecker, T. L., Aneshansley, D. J. and Beyenbach, K. W. (1992). Unique electrophysiological effects of dinitrophenol in Malpighian tubules. *Am. J. Physiol.* **263**, R609–R614.

Pannabecker, T. L., Hayes, T. K. and Beyenbach, K. W. (1993). Regulation of epithelial shunt conductance by the peptide leucokinin. *J. Membr. Biol.* **132**, 63–76.

Peng, S. B., Li, X., Crider, B. P., Zhou, Z., Andersen, P., Tsai, S. J., Xie, X. S. and Stone, D. K. (1999). Identification and reconstitution of an isoform of the 116-kDa subunit of the vacuolar proton translocating ATPase. *J. Biol. Chem.* **274**, 2549–2555.

Plawner, L., Pannabecker, T. L., Laufer, S., Baustian, M. D. and Beyenbach, K. W. (1991). Control of diuresis in the yellow fever mosquito *Aedes aegypti*: Evidence for similar mechanisms in the male and female. *J. Insect Physiol.* **37**, 119–128.

Sawyer, D. B. and Beyenbach, K. W. (1985). Dibutyryl-cAMP increases basolateral sodium conductance of mosquito Malpighian tubules. *Am. J. Physiol.* **248**, R339–R345.

Ussing, H. H. and Windhager, E. E. (1964). Nature of shunt pathway and active sodium transport path through frog skin epithelium. *Acta Physiol. Scand.* **61**, 484–504.

Weltens, R., Leyssens, A., Zhang, S. L., Lohrmann, E., Steels, P. and Van-Kerkhove, E. (1992). Unmasking of the apical electrogenic proton pump in isolated Malpighian tubules *Formica polyctena* by the use of barium. *Cell. Physiol. Biochem.* **2**, 101–116.

Wieczorek, H. (1992). The insect V-ATPase, a plasma membrane proton pump energizing secondary active transport: molecular analysis of electrogenic potassium transport in the tobacco hornworm midgut. *J. Exp. Biol.* **172**, 335–343.

Wieczorek, H., Gruber, G., Harvey, W. R., Huss, M. and Merzendorfer, H. (1999). The plasma membrane H^+-V-ATPase from tobacco hornworm midgut. *J. Bioenerg. Biomembr.* **31**, 67–74.

Wieczorek, H., Putzenlechner, M., Zeiske, W. and Klein, U. (1991). A vacuolar-type proton pump energizes K^+/H^+ antiport in an animal plasma membrane. *J. Biol. Chem.* **266**, 15340–15347.

Yonath, J. and Civan, M. M. (1971). Determination of the driving force of the sodium pump in toad bladder by means of vasopressin. *J. Membr. Biol.* **5**, 366–385.